TABLE 1 Commonly used MALDI matrices for imaging of biomolecules in tissue samples

Matrix	Applications	References
2,5-Dihydroxybenzoic acid (DHB)	Lipids, Sugars, peptides, nucleotides, glycopeptides, glycoproteins, and small proteins	Fournier *et al.* (2003); Herring *et al.* (2007); Tholey and Heinzle (2006)
α-Cyano-4-hydroxycinnamic acid (CHCA)	Peptides, small proteins and glycopeptides	Schwartz *et al.* (2003); Tholey and Heinzle (2006)
2,6-Dihydroxyacetophenone (DHA)	Phospholipids	Jackson *et al.* (2005); Seeley *et al.* (2008); Tholey and Heinzle (2006)
2,4,6-Trihydroxyacetophenone (THAP)	Lipids	Stuebiger and Belgacem (2007)
p-nitroaniline (PNA)	Phospholipids	Estrada and Yappert (2004); Rujoi *et al.* (2004)
2-mercaptobenzothiazole (MBT)	Phospholipids	Astigarraga *et al.* (2008)
Sinapinic acid (SA)	Peptides and large proteins	Schwartz *et al.* (2003)
CHCA/aniline, ionic matrix	Peptides	Lemaire *et al.* (2006b)
CHCA/n-butylamine, ionic matrix	Phospholipids	Shrivas *et al.* (2010)

phospholipids (Herring *et al.*, 2007; Seeley *et al.*, 2008). A great variety of matrices are used for the analysis of biomolecules, some of which are listed in Table 1.

3.2.1. Ionic Matrices for IMS

Ionic matrices (IMs) constitute a new class of organic matrices reported for the analysis of a number of different molecules in MALDI-MS. IMs are good for MALDI-MS imaging studies due to the fact that the process solubulizes several analytes, has vacuum stability, and forms homogenous crystals with analyte molecules. IMs have been used to obtain enhanced sensitivity and good reproducibility in the analysis

of biomolecules (Armstrong *et al.*, 2001; Laremore *et al.*, 2007). IMs such as 2,5-dihdroxybenzoic acid butylamine (DHBB) and α-cyno-4-hydroxycinnamic acid butyl amine (CHCAB) render good crystal formation, signal intensity, and reproducibility compared with conventional matrices such as DHB and CHCA (Shrivas *et al.*, 2010). The results are

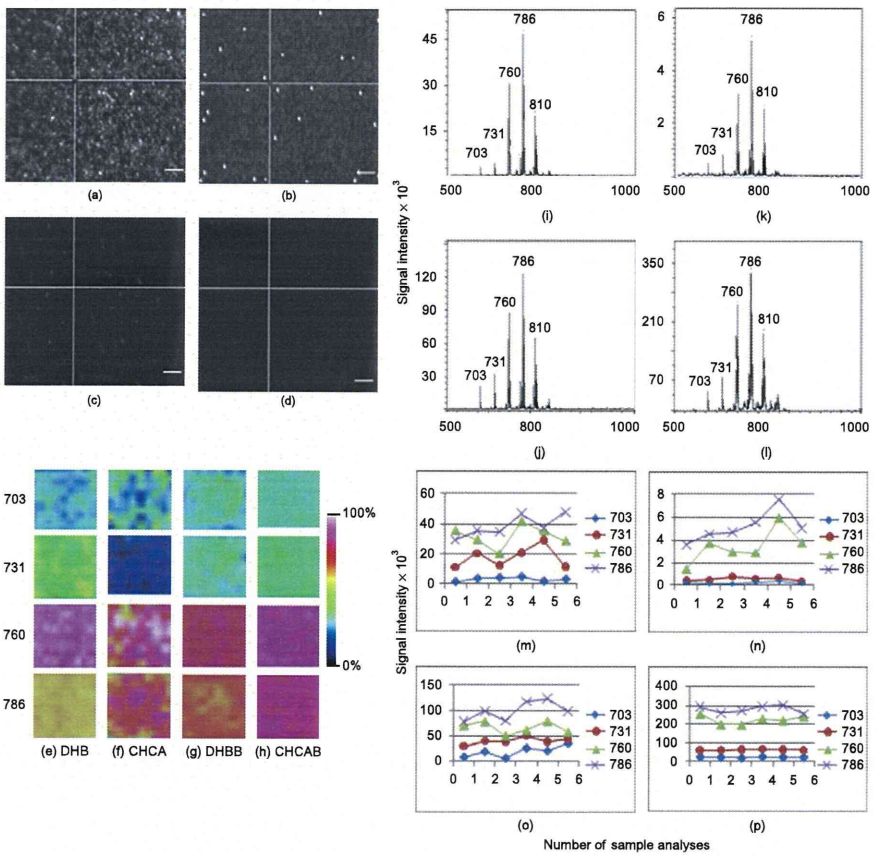

FIGURE 6 The crystal formation of (a) DHB, (b) CHCA, (c) DHBB, and (d) CHCAB matrixes with phospholipids on to a MALDI target plate. The pictures were taken with an Ultraflex II TOF/TOF. The scale bar (white color line) is 100 μm; images (e) to (h) show the ion image of phospholipids reconstructed obtained by using (e) DHB, (f) CHCA, (g) DHBB, and (h) CHCAB matrix at *m*/*z* 703, 731, 760, and 786. Images (i) to (l) show the signal enhancement: 3- to 7-fold enhancement of signal intensity when DHBA IM (image i) is used as a matrix compared with DHB matrix (image j) and 50- to 100-fold improvement of signal intensity using CHCAB IM (image k) compared with CHCA matrix (image l). Graphs (m) to (p) show the six replicate analyses of samples with ± relative standard deviation, % by using (m) DHB: ± 20.5–40.8%, (n) CHCA: ± 29.5–45.8%, (o) DHBB: ± 14.5–21.8%, and (p) CHCAB: ± 7.5–10.0%. Reprinted from Shrivas *et al.* (2010) with permission from American Chemical Society.

shown in Figure 6. Direct tissue analyses of peptides in rat brain tissue sections using IMs improved the ionization efficiency and increased the signal intensity of ion images of molecules compared with the conventional matrix (Lemaire *et al.*, 2006a). IMs were also used for imaging and identification of gangliosides in mouse brain (Chana *et al.*, 2009). DHB and CHCAB IMs in MALDI-IMS were also used for analysis of mouse liver and cerebellum tissues to identify the different species of lipids; results with CHCAB were better than with conventional matrices (DHB and CHCA).

3.2.2. Nanoparticles as Matrices for IMS

In addition, nanoparticles (NPs) can be used as a matrix instead of organic matrices for the analysis of low-molecular-weight molecules (< 500 Da). One problem with the organic matrix ions is that they themselves produce an intense peak in the mass spectrum and hence suppress detection of the analyte of interest, which then obviously decreases the sensitivity of the method. To circumvent this disadvantage, nanomaterials and inorganic compounds have been introduced. The Tanaka and Sunner groups investigated the application of cobalt powder (NPs) and graphite microparticles, respectively, suspended in glycerol to analyze proteins and/or peptides in MALDI-MS analyses. The use of NPs as a matrix in MALDI-MS allows for efficient absorption of laser energy as well as efficient subsequent desorption and ionization of molecules from the sample surface (Sunner *et al.*, 1995; Tanaka *et al.*, 1988). Desorption/ionization on porous silicon (DIOS) is another matrix-free method that is produced by etching of the silicon surface. Small molecules can be efficiently ionized using DIOS as an effective surface (Wei *et al.*, 1993). Today nanomaterial surfaces are also applied for the direct analysis of tissue samples in MALDI-IMS. Northen's group introduced a new nanostructure surface for imaging of biomolecules in tissue samples known as ionization nanostructure-initiator mass spectrometry (NIMS) (Northen *et al.*, 2007). Several other sample preparation procedures, such as graphite-assisted laser desorption/ionization (GALDI) (Cha and Yeung, 2007), nano-assisted laser desorption/ionization (NALDI) (Vidova *et al.*, 2010), and DIOS have been proposed for imaging of biomolecules in tissue samples. Taira *et al.* (2008) developed another matrix-free method called nanoparticle-assisted laser desorption/ionization imaging mass spectrometry (Nano-PALDI-IMS) that can be used to visualize peptides, phospholipids, and metabolites in tissue sections. Recently silver (Hayasaka *et al.*, 2010) and gold (Goto-Inoue *et al.*, 2010a) NPs were applied for imaging and identification of fatty acids and glycosphingolipids, respectively, an analysis that could be difficult to perform by conventional MALDI-MS using DHB as a matrix. Figure 7 demonstrates imaging and identification of fatty acids from mouse liver sections using silver NPs as a matrix (Hayasaka *et al.*, 2010). More recently, TiO_2 NPs were applied for the analysis of low-molecular

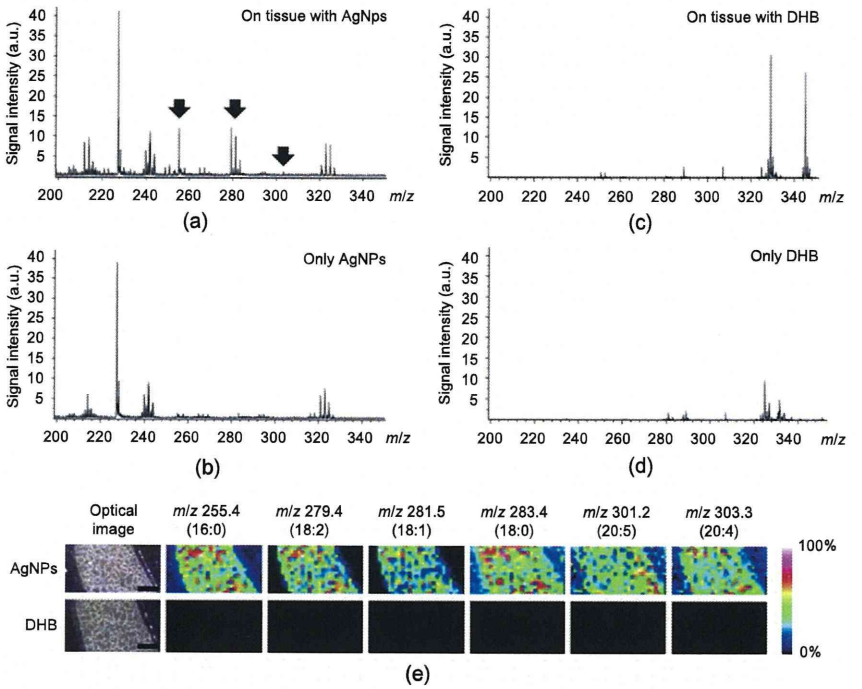

FIGURE 7 Identification of fatty acids from mouse liver sections in nano-PALDI-IMS. The serial sections were sliced to a thickness of 10 μm. Silver nanoparticles (NPs) or DHB matrix solution was sprayed on the surface of the mouse liver sections, respectively. Their sections were measured with a scan pitch of 100 μm by nano-PALDI-IMS analysis in negative-ion mode. The mass spectra were obtained from the sections sprayed with silver NPs (a) on tissue section, (b) only silver NPs or DHB matrix, (c) on tissue section, and (d) only DHB solution. The peaks used to reconstruct the ion image are indicated by arrows. (e) In the analysis using silver NPs and DHB, the ion signals at m/z 255.4 (16:0), 279.4 (18:2), 281.5 (18:1), 283.4 (18:0), 301.2 (20:5), and 303.3 (20:4) were detected. The scale bars are 500 μm. Reprinted from Hayasaka *et al.* (2010) with permission from Springer.

weight-biomolecules in mouse brain without observing any NP-related peaks. More individual signals and higher intensity were obtained when TiO_2 NPs were used as a matrix compared with a DHB matrix (Shrivas *et al.*, 2011). Thus we can conclude that the use of a nanomaterial surface is efficient and effective for desorption and ionization of molecules; the process yields images with higher resolution.

3.3. Application of Matrix Solution

The deposition of matrix solution on the surface of a tissue section is another important step in obtaining homogeneity, reproducibility, and good resolution of the biomolecule. The matrix solution consists of three

components—organic solvent, matrix, and trifluoroacetic acid (TFA). Crystal formation is affected by the concentration of matrix and the ratio of organic solvent to water; organic solvent is used to dissolve the solid matrix and extract the molecules from the tissue section. This extraction is followed by crystal formation on the surface of the tissue section. The addition of TFA provides free protons for effective ionization of the analytes, and typically, singly charged $[M + H]^+$ ions are formed. A number of devices are useful for the deposition of matrix solution on the surface of tissue sections—for example, chemical inkjet printer spotter (Baluya *et al.*, 2007), robotic spotting depositors (Aerni *et al.*, 2006), electrospray depositors (Altelaar *et al.*, 2007), and airbrush sprayers (Hayasaka *et al.*, 2009). The sublimation (Hankin *et al.*, 2007) and stainless steel sieve (Puolitaival *et al.*, 2008) methods have demonstrated good signal intensity and sample reproducibility. Figure 8 shows a thin layer chromatography (TLC) sprayer (image a), sublimation apparatus (b), air brush sprayer (c), and a chemical inkjet printer (d) used for matrix deposition. The goal of these matrix deposition approaches is to improve the homogeneity of the sample surface and enhance the signal intensity for the identification of biomolecules compared with direct deposition of the matrix.

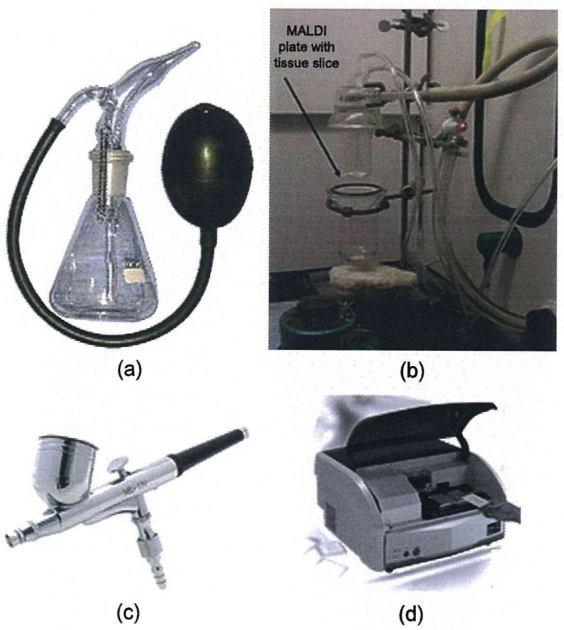

FIGURE 8 Apparatus used to deposit matrix on the tissue section. (a) Thin-layer chromatography sprayer, (b) sublimation apparatus, (c) air brush sprayer, and (d) chemical inkjet printer. Reprinted from Hankin *et al.* (2007) with permission from Springer.

4. INSTRUMENTATION

4.1. Quadrupole Mass Analyzer

A quadrupole mass analyzer is made from four parallel rods maintained at fixed direct current (DC) with an alternating radiofrequency (RF). With this setup molecular ions formed at the source pass through the middle of the quadrupoles in the electric field region and the ions of a specific m/z have a stable trajectory path and may pass all the way to the detector, while the remaining ions collide with the electrodes and never reach the detector (Gross, 2004). Using a continuous and controlled manner to change the frequency and potential, the quadropole transmits molecules at certain m/z values. Figure 9a shows a diagram of quadrupole mass analyzer. The sensitivity of the instrument can be enhanced by increasing the number of qaudupoles from two to three (triple quadrupole) in series. In triple-quadrupole analyzers, the first (Q_1) and third (Q_3) quadrupoles act as filters, and the second (Q_2) quadrupole functions as a collision cell. The third (Q_3) quadrupole is worked at normal RF/DC or in the linear ion trap (LIT) mode (Douglas *et al.*, 2005). Hopfgartner *et al.* (2009) demonstrated the fast imaging of complete rat sections using MALDI coupled with a triple-quadrupole LIT where the precursor ion mode can be used to monitor the presence of the parent drug in the tissue section.

4.2. Time-of-Flight Mass Analyzer

The TOF-MS analyzer has become valuable for direct analysis of biomolecules from tissue samples. In TOF-MS, the different masses of ions are separated based on their differences in travel time through a drift region. The lighter ions produced from the source travel faster at the end of the drift region compared with heavier ions in the tube (see Figure 9b). However, TOF-MS has disadvantages in mass accuracy, resolving power, and its inability to perform tandem MS experiments (Goto-Inoue *et al.*, 2011; Gross, 2004). This drawback has been overcome by the introduction of an orthogonal geometry (oTOF)-MS analyzer to extract pulsed ions from a continuous ion beam. Huang *et al.* (2011) investigated the use of oTOF-MS for imaging and simultaneous detection of metal and nonmetal elements in tissue section with spatial resolution of 50 μm.

Ion mobility (IM) spectrometry can also be coupled with the TOF-MS system for direct analysis of tissue samples. The instrument has oTOF-MS and is equipped with an IM spectrometer located between the quadrupole and the TOF-MS analyzer. The IM spectrometer separates ions based on their IM (i.e., their shape) and TOF-MS separates ions according to their m/z ratio in the MS (Verbeck *et al.*, 2002). Separation of structurally similar

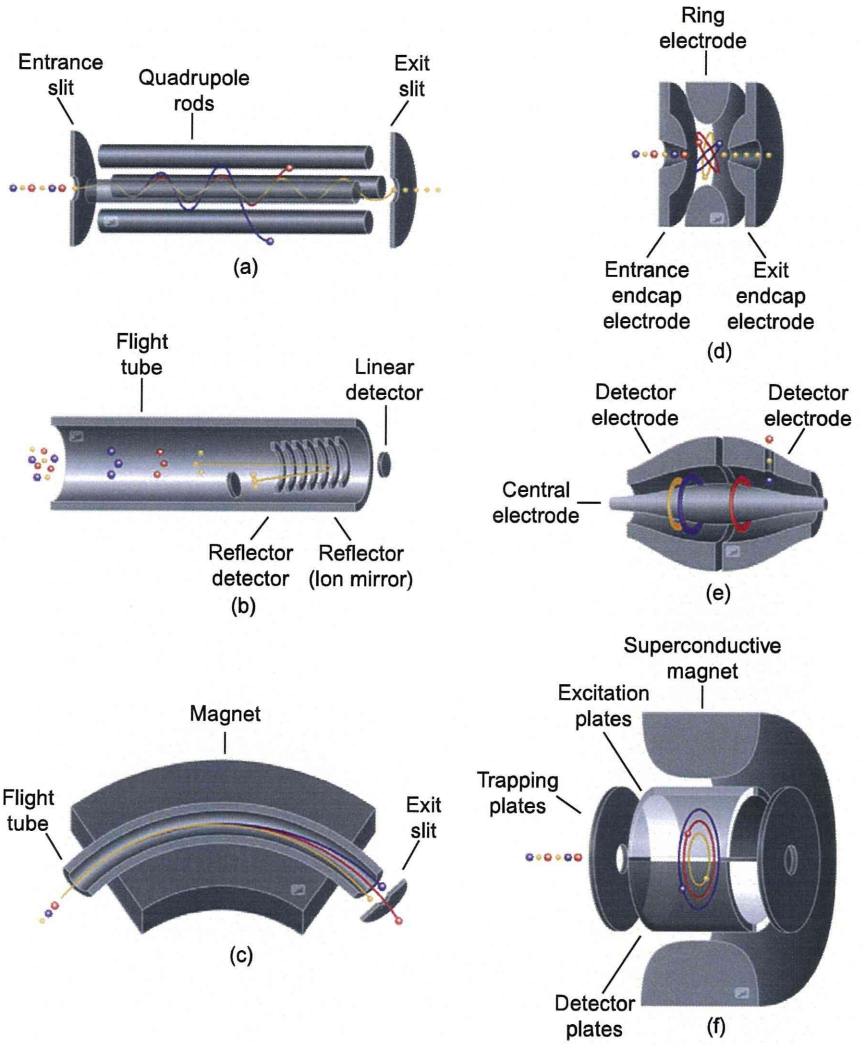

FIGURE 9 Schematic description of six mass analyzers used in mass spectrometers. (a) Quadrupole, (b) time-of-flight, (c) magnetic sector, (d) ion trap, (e) orbitrap, (f) ion cyclotron resonance. Reprinted from Pol *et al.* (2010) with permission from Springer.

ions and ions of the same charge state is thus possible through their different mobility in the IM spectrometer. The combined techniques of IM and TOF-MS were used for imaging and identification of digested proteins. IM separates isobaric ions that cannot be distinguished by MALDI-TOF alone, providing mass- and time-selected ion images of biomolecules in tissue samples (Stauber *et al.*, 2010).

In addition, the combination of a quadrupole (Q) mass analyzer with a TOF-MS is called a Q-TOF-MS system and is used for structural analysis with tandem MS. The localization of a xenobiotic substance in skin has been reported by applying a Q-TOF-MS (Bunch *et al.*, 2004). Another approach for imaging and identification of molecules is the combination of two TOF mass analyzers; this hybrid is called TOF/TOF. First, TOF-MS separates precursor ions using a velocity filter; second, TOF-MS analyzes the fragment ions (Gross, 2004). MALDI-TOF/TOF is a simple, rapid, and sensitive technique for MALDI imaging of biomolecules in tissue sections (Hayasaka *et al.*, 2010; Sugiura *et al.*, 2009).

4.3. Sector-Type Mass Analyzer

The sector mass spectrometer consists of large electromagnetic ("B" sector) and electrostatic focusing devices ("E" sector) that, depending on the different manufacturers' use, differ in their geometries (Cottrell and Greathead, 1986). The motion of the ions in the trajectory pathway depends on the strength of electric and magnetic field where each ion (m/z) travels with different speeds (see Figure 9c). Magnetic sectors are used for high-resolution elemental imaging and identification of samples in combination with dynamic SIMS. The magnetic sector and several movable detectors allow a simultaneous detection of several elements or small molecules (within a narrow mass range) with higher sensitivity. Slodzian *et al.* (1992) used a SIMS coupled with a magnetic sector double-focusing mass spectrometer for simultaneous imaging of several elements in tissue sample.

4.4. Ion Trap Mass Analyzer

A quadrupole ion trap (QIT or 3D-IT) operates in a 3D quadrupole field maintained at constant DC and RF fields to trap the moving ions of m/z range. A QIT consists of three hyperbolic-shaped electrodes: the central ring electrode and two adjacent end cap electrodes (entrance and exit) (see Figure 9d). A 3D-IT is a small, relatively inexpensive instrument for sensitive analysis; it can also be used for MS^n analysis of molecules in the tissue samples (Gross, 2004; Hopfgartner *et al.*, 2004). Shimma *et al.* (2008) reported their use of a MALDI-QIT–TOF-MS instrument for imaging of phospholipids, glycolipids, and tryptic-digested proteins. MS analyses were performed to confirm their presence. Recently a mass microscope coupled with a high-resolution atmospheric pressure-laser desorption/ionization (AP-MALDI) and QIT-TOF was used for imaging and identification of volatile substances in ginger (Harada *et al.*, 2009). This instrument allows researchers to precisely determine the

specific tissue section prior to IMS and has spatial resolution (10 μm) higher than the naked eye.

In a linear quadrupole ion trap (LIT) or 2D traps (2D-IT), the ions are trapped in a 2D quadrupole field and then pass axially. The 2D-IT ion trap produces reasonable mass accuracy, mass resolution, and sensitivity (Schwartz *et al.*, 2002). LIT has a better ion storage capacity and a higher trapping efficiency compared with 3D-IT. However, the disadvantage of LIT is the relatively narrow mass range of small molecule analysis. Garrett *et al.* (2007) described a new MALDI-LIT-MS for imaging of tissue samples and also used for MS^n analyses to confirm the molecules. Enomoto *et al.* (2011) demonstrated the visualization of phosphatidylcholine (PC), lysophosphatidylcholine, and sphingomyelin in mouse tongue using LTQ (linear trap quadrupole)-MALDI-IMS (Enomoto *et al.*, 2011).

4.5. Orbitrap Mass Analyzer

In an orbitrap mass analyzer, the ions are rotated around a central electrode by applying an appropriate voltage between the outer and central electrodes. Hence, the ions of a specific m/z ratio cycle in rings that oscillate around the central spindle and then pass through the detector (Makarov *et al.*, 2006). Figure 9e shows the overview of the orbitrap mass analyzer. LTQ-Orbitrap has been used to analyze compounds with high resolving power and excellent mass accuracy that appreciably decrease false-positive peptide identifications in the sample (Adachi *et al.*, 2006; Makarov *et al.*, 2006). Verhaert *et al.* (2010) demonstrated the use of LTQ-orbitrap for imaging of neuropeptides in neural tissue samples. In addition, it has also been used for identification and sequencing of neuoropeptides from neural tissue using MALDI-MS with an ion trap–orbitrap hybrid instrument. Landgraf *et al.* (2009) showed the high resolution and accurate measurement of ion images of lipids in spinal cord using MALDI-LIT–orbitrap-MS. Manicke *et al.* (2010) demonstrated imaging of lipids in rat brain tissue section with a high-resolving power instrument of DESI-LTQ–orbitrap-MS.

4.6. Ion Cyclotron Resonance Mass Analyzer

In an ion cyclotron resonance (ICR)-MS analyzer, the ions of a particular m/z ratio are isolated based on the cyclotron frequency of the ions in a constant magnetic field. The oscillation of ions in ICR induces an alternating current that is equivalent to their m/z ratios. Figure 9f shows the schematic for an ICR analyzer. Fourier transforms (FT)-ICR-MS continues to deliver the highest mass-resolving power and mass measurement accuracy (Gross, 2004). The combination of MALDI-TOF-MS with the FT-ICR-MS technique is useful for high–spatial resolution analysis and

identification of unknown biomolecules in tissue samples. Thus the high mass resolution of the FT-ICR-MS can be used to analyze compounds that cannot be distinguished with lower–mass resolution mass spectrometers (Taban *et al.*, 2007; Wang *et al.*, 2011). MALDI-FT-ICR has also been reported for IMS analysis of drugs and metabolites in tissue. The accurate mass measurement can be performed using FT-ICR-MS, which provided a molecular specificity for the ion images obtained from tissue sample analysis (Cornett *et al.*, 2008).

5. IMS MEASUREMENTS

MALDI-IMS experiments can be performed after the deposition of matrix on the tissue section and using different types of MS instruments as discussed above. The setting of the laser energy, detector gain, and random walk function are optimized in order to obtain better signal intensity of the target molecules during the IMS analysis. Either a particular region of the tissue or the entire tissue section is selected for analysis, depending on the particular interest. At present, the commercially available instruments can perform IMS analyses with the highest spatial resolution of $\sim 25\,\mu m$ (Goto-Inoue *et al.*, 2009a). Recently we developed a mass microscope that can move a sample stage by $1\,\mu m$, and the finest size of the laser diameter is approximately $10\,\mu m$ (Harada *et al.*, 2009). The measurement time of IMS experiments depends on the number data spots, the frequency of the laser, and the number of shots per spot.

6. DATA ANALYSIS

Due to the large (gigabytes) size of the dataset, high-capacity visualization software is required to visualize the ion image and distribution pattern of biomolecules in tissue samples. New computing methods are required for both rapid, accurate data acquisition and the interpretation of the IMS analysis results. Therefore, in addition to instrumental improvements, data acquisition and software development have been important for the production of reliable data. The databases used are based on algorithms that perform analysis through statistical evaluation of observed and theoretical spectra of bimolecules. BioMap (http://www.maldi-msi.org, Novartis, Basel, Switzerland) and flexImaging (http://www.bdal.com, Bruker Daltonics GmbH, Bremen, Germany) imaging software are used to identify biomolecules in various sample types. The intensity of the different color images obtained by both software packages can relate the distribution of biomolecules in the tissue section. These software packages also help in understanding the localization of biomolecules at

particular regions of interest (ROIs) for mass spectral comparison and other statistical analysis.

BioMap imaging software can be used for different instruments such as PET, nuclear magnetic resonance (NMR), computed tomography (CT), and near-infrared fluorescence (NIRF) as the result of multiple modifications. Interactive data language Virtual Machine (Research Systems, Boulder, CO) is required in the system to process the data obtained from IMS analysis. BioMap software can also be used for baseline correction, spatial filtering, and averaging of spectra for presentation of the IMS results.

The flexImaging software is used for the acquisition and evaluation of MALDI-TOF imaging results. The mass peaks (at m/z) obtained in the mass spectrum are normalized to total ion current and then the peak intensity is taken into account to study the molecules distribution on the tissue section. The imaging MS experiments are performed by collecting spectra at a resolution of 50 to 400 μm in the same m/z range as above. Principal component analysis (PCA) is an unsupervised statistical method used to identify groups of closely correlated variables; for MS imaging datasets these variables are spatial coordinates and mass. This approach also reduces the multidimensional datasets to the lower dimensions (Chou, 1975). PCA analysis is performed using ClinProTools 2.1 software (Bruker Daltonics). Zaima *et al.* (2009) performed a PCA for screening of metabolites in the fatty liver. Several differences were found in identifying the metabolites in fatty and normal liver tissue samples. PCA was also used in proteomics studies (Deininger *et al.*, 2008; Djidja *et al.*, 2010; Yao *et al.*, 2008).

7. APPLICATIONS OF IMS FOR DIRECT ANALYSIS OF TISSUE

7.1. IMS for Lipidomics

Lipids are the main constituents of cell membranes; the major functions of lipids are transportation of ions and signals across the cell membrane. Various types of lipids, such as glycerophospholipids (GPLs), sphingolipids, sterol lipids, saccharolipids, waxes, and fat-soluble vitamins are found in biological systems. Membranes act as barriers to separate compartments within eukaryotic cells and to separate all cells from their surroundings (Brown, 2007; Fahy *et al.*, 2009; Lee *et al.*, 2003). The identification and quantification of lipids in tissue sample can help in understanding several biosynthetic and metabolic pathways that govern human diseases, such as insulin-resistant diabetes, Alzheimer's disease, schizophrenia, cancer, atherosclerosis, and infectious diseases (Oresic *et al.*, 2008). Thus the analysis of lipids in tissue samples is a very important issue. High-performance liquid chromatography (HPLC) (McCluer *et al.*, 1986), TLC (Touchstone,

1995), and MS have been used to analyze lipids in tissue samples. However, the sample preparation procedures in chromatographic techniques are lengthy and the localization of biomolecules in tissue sample surface cannot be established. Therefore, different IMS systems are successfully used for imaging of lipids. The analysis of glycerophospholipids, sphingolipids, and neutral lipids is discussed in detail in the following sections.

7.1.1. Glycerophospholipids

GPLs are glycerol-based phospholipids and essential components of cell membranes. They act as second messengers involved in cell proliferation, apoptosis, and metabolism. The determination of GPL content in tissue samples is useful for finding potential biomarkers for diseases such as atherosclerosis or rheumatism (Fuchs *et al.*, 2005; Schmitz and Ruebsaamen, 2010). Altered levels of lipids are found in many pathological conditions such as Alzheimer's disease (Han *et al.*, 2001, 2002), Down syndrome (Murphy *et al.*, 2000), diabetes (Han *et al.*, 2007), and Niemann–Pick disease (He *et al.*, 2002). Figure 10 illustrates the basic structures of common classes of GPLs such as PC, phosphatidylethanolamine (PE), phosphatidylinositol (PI), and phosphatidylserine (PS) (Jackson and Woods, 2009). PC is easily ionized due to its charged quaternary ammonium head group and has thus become a popular lipid species to investigate (Pulfer and Murphy, 2003). The ionized molecules observed in the mass spectrum are usually either protonated $[M+H]^+$, sodiated $[M+Na]^+$, or pottasiated $[M+K]^+$ in positive-ion mode. Phospholipids such as PE, PS, PA, PG, and PI may generate negative ions due to the presence of the phosphodiester moiety and display molecular anions $[M-H]^-$ (Fuchs *et al.*, 2010). The addition of potassium acetate (Sugiura *et al.*, 2009) or LiCl (Jackson *et al.*,

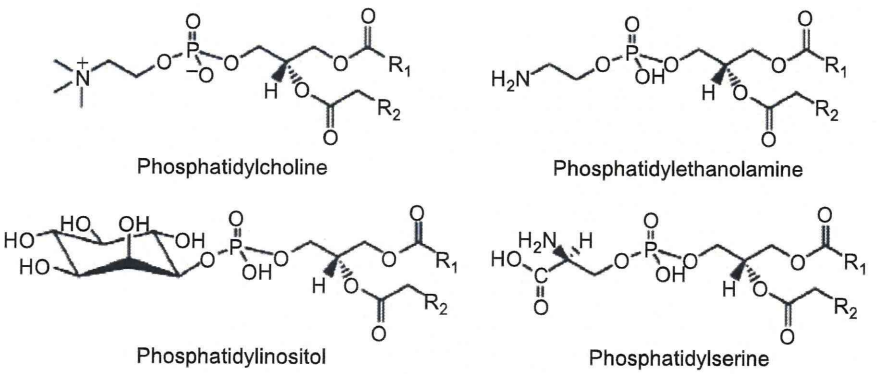

FIGURE 10 Structure of glycerophospholipids. Reprinted from Jackson and Woods (2009) with permission from Elsevier Science.

2005) to the matrix solution has also been reported for effective ionization of molecules in tissue samples.

The selection of MALDI matrices is an important issue. For MALDI-IMS, the matrix should have good vacuum stability and homogenous crystal formation containing analyte molecules. Various matrices have been reported for the identification and characterization of lipids in MALDI-MS, including DHB (Petkovic *et al.*, 2001; Puolitaival *et al.*, 2008; Schiller *et al.*, 1999), DHA (Jackson *et al.*, 2005; Shimma *et al.*, 2007), p-nitroaniline (PNA) (Estrada and Yappert, 2004; Rujoi *et al.*, 2004), and 9-aminoacridine (Eibisch and Schiller, 2011; Teuber *et al.*, 2010). However, PNA and dihydroxyacetone phosphate (DHAP) were unstable under high vacuum conditions and started to evaporate after their introduction into the MALDI-MS instrument (Jackson *et al.*, 2005; Rujoi *et al.*, 2004; Shrivas *et al.*, 2010). DHB matrix exhibited a lower sensitivity for the detection of PA, PS, PE, PI, and PG in negative-ion mode, possibly due to its acidity (Estrada and Yappert, 2004; Petkovic *et al.*, 2001). DHA can be used in both positive and negative ionization modes for analysis of phospholipids (Woods *et al.*, 2006). PNA is another good matrix for the analysis of phospholipids in either positive-ion or negative-ion modes (Estrada and Yappert, 2004). Recently, 2-mercaptobenzothiazole (MCT) was added as an alternative to the use of DHB for MALDI-MS analysis of phospholipids in brain and liver tissue samples (Astigarraga *et al.*, 2008). The main advantages of MCT over the commonly used matrices DHB, DHA. and PNA are low vapor pressure, low acidity, and homogenous crystal formation, which allowed for detection of more lipid species in negative mode, with high sensitivity and high detection reproducibility. Ionic matrices have also been used in MALDI-IMS owing to the good vacuum stability, homogenous crystal formation, and good solubility of analytes for efficient ionization and desorption of molecules (Chana *et al.*, 2009; Lemaire *et al.*, 2006a; Shrivas *et al.*, 2010). Shrivas *et al.* (2010) used an ionic matrix of CHCAB to image and identify lipids in mouse cerebellum and found that this ionic matrix yields a higher number of ion images compared with the use of DHB matrix in MALDI-IMS (Figure 11). Use of NPs is another good approach for selective and sensitive analysis of lipids and small metabolites in tissue samples without matrix-oriented peaks in the low-molecular-mass range (Cha and Yeung, 2007; Goto-Inoue *et al.*, 2010a; Hayasaka *et al.*, 2010; Shrivas *et al.*, 2011; Taira *et al.*, 2008).

Sugiura *et al.* (2009) showed the imaging of polyunsaturated fatty acid–containing PC in mouse brain using MALDI-IMS. The results demonstrated that arachidonic acid (AA) and DHA-containing PC were found in the hippocampal neurons and cerebellar Purkinje cells, respectively. Figure 12 shows the localization of PC species in different layers of the mouse brain (Sugiura *et al.*, 2009). The distribution of PC species also has been reported in the mouse retinal section via MALDI-IMS analysis. The localization of PC (16:0/18:1) was found in the inner nuclear layer and

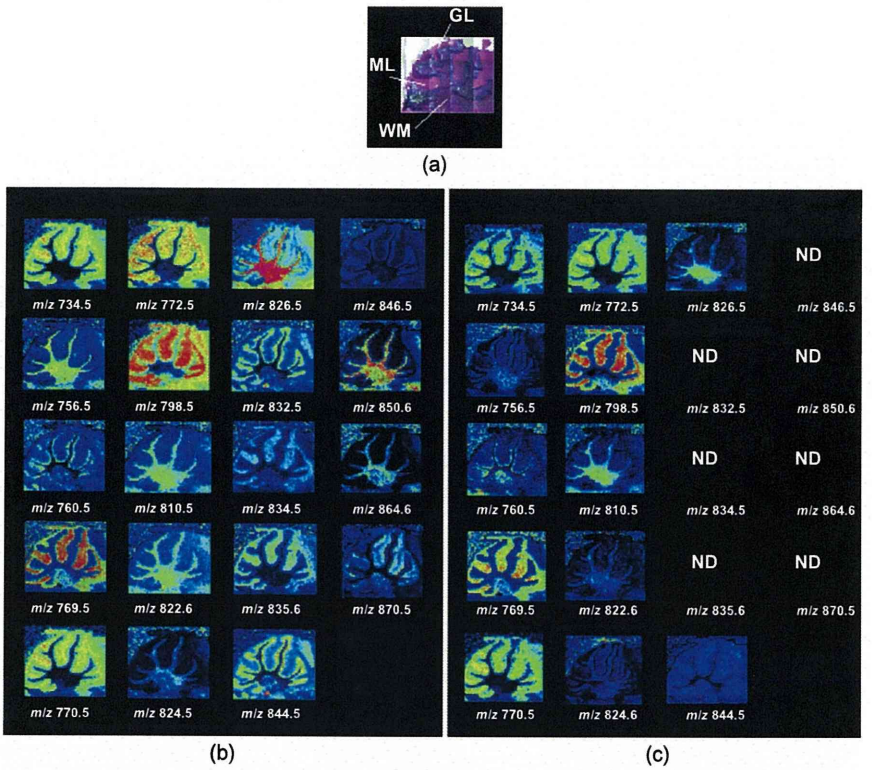

FIGURE 11 (a) H&E-stained mouse cerebellum showing three layers with 1.5-mm scale bar (white color). The ion images of lipids in mouse cerebellum tissue section obtained by using (b) CHCAB and (c) DHB as a matrix at m/z 734.5 $[(PC(16:0/16:0)+H)]^+$, 770.5 $[PC(16:0/16:1)+K]^+$, 772.5 $[PC(16:0/16:0)+K]^+$, 798.5 $[PC(16:0/18:1)+K]^+$, 834.5 $[PC(18:0/22:6)+H]^+$, and 870.5 $[PC(18:1/22:6)+K]^+$ were localized in the molecular layer of cerebellum; at m/z 760.5 $[PC(16:0/18:1)+H]^+$, 832.5 $[PC(18:0/20:4)+Na]^+$, 844.5 $[PC(16:0/22:6)+K]^+$, and 846.5 $[PC(18:1/20:4)+K]^+$ were specific to the granular layer; and at m/z 756.50 $[PC(16:0/16:0)+Na]^+$, 810.5 $[PC(18:0/18:1)+Na]^+$, 824.5 $[PC(18:0/18:2)+K]^+$, and 826.5 $[PC(18:0/18:1)+K]^+$ and were found to be concentrated in the white matter of cerebellum. The ion images *at* m/z 769.5 $[SM(d18:1/18:0)+K]^+$ and 835.6 $[SM(d18:1/24:1)+Na]^+$ illustrated that the molecules were distributed in the region of molecular layer of tissue. The ion images at m/z822.6 $[GalCer(d18:1/22:0)+K]^+$ and 850.6 $GalCer(d18:1/24:0)+K]^+$ were localized in the white matter of mouse cerebellum. ND indicates the molecules were not detected. GL, granular layer; ML, molecular layer; WM, white matter. Reprinted from Shrivas *et al.* (2010) with permission from American Chemical Society.

the outer plexiform layer; PC (16:0/16:0) in the outer nuclear layer and inner segment; and PC (16:0/22:6) and PC (18:0/22:6) in the outer segment and pigment epithelium (Hayasaka *et al.*, 2008). Differential localization of PC (16:0/20:4) species was observed between terminal and stem villi of

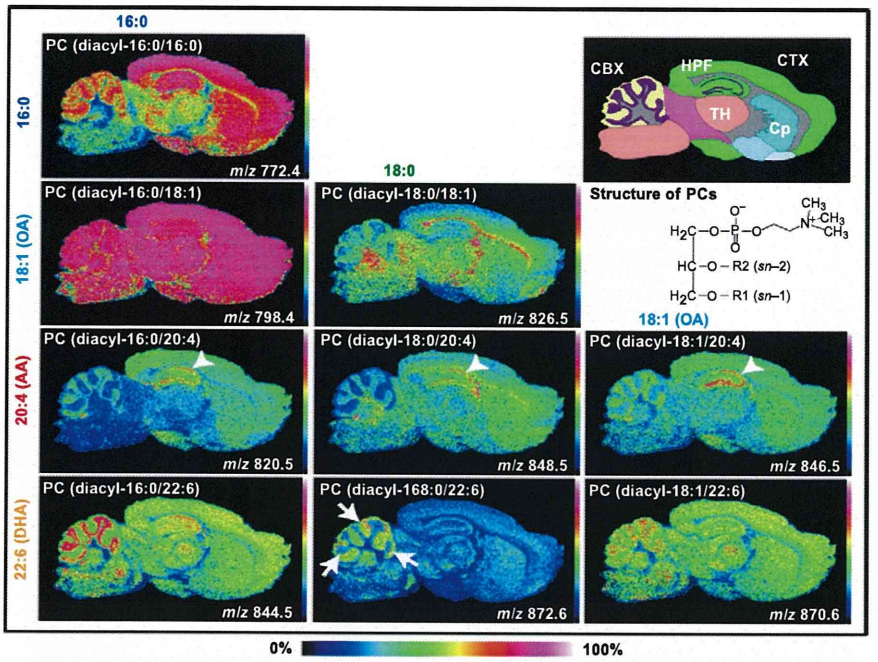

FIGURE 12 Identification of molecular species of PC in sagittal mouse brain sections by MALDI-IMS. Among the PC, AA-PC showed characteristic localization in the hippocampal cell layers (arrowheads). Among DHA-containing species, two abundant species, PC (diacyl-16:0/22:6) and PC (diacyl-18:1/22:6), were commonly enriched in the granule layer of the cerebellum, while PC (diacyl-18:0/22:6) showed a characteristic dotted distribution pattern near the cell layer (arrows). CBX, cerebellar cortex; CP, corpus striatum; CTX, cerebral cortex; HPF, hippocampal formation; TH, thalamus. Reprinted from Sugiura *et al.* (2009) with permission from the American Society for Biochemistry and Molecular Biology.

human placenta, which could be helpful in understanding the pathological involvement of fetal growth restriction and fetal hypoxia (Kobayashi *et al.*, 2010). The accumulation of lipid molecules, such as LPC (1-acyl 16:0), PC (1-acyl 36:4), and shingomyelin (SM) (d18:1/16:0) around the damaged valvular region was investigated and suggested an association of these molecules with tissue inflammation and resultant valvular incompetence (Tanaka *et al.*, 2010). PC (diacyl-16:0/20:4) containing an AA was found at higher concentration in prefrontal cortex tissue compared with occipital cortex tissue in the brains of patients with schizophrenia (Matsumoto *et al.*, 2011). The specific localization of five PC species in the cochlea was also examined using the mass microscope. A differential distribution of PC species was observed; (16:0/18:1) in the organ of Corti and the stria vascularis, (16:0/18:2) in the spiral ligament, and (16:0/16:1) in the organ of Corti (Takizawa *et al.*, 2010). Recently Goto-Inoue *et al.* (2009a)

investigated use of a TLC-Blot-MALDI-IMS for analysis and characterization of acidic, neutral glycosphingolipids and PC in sample mixtures. In TLC-Blot, the lipids are separated and transferred to a polyvinylidene fluoride (PVDF) membrane without any change in the stability of the molecules. PVDF membranes with the sample may then be placed on the target plate for MALDI-IMS analysis. This method might be useful for the detection of minor components that could not be detected by the conventional TLC method. SIMS is also used for imaging of lipids at high spatial resolution and sensitive detection. The combined approaches of MALDI-IMS and SIMS-IMS have been used for imaging of PC in cultured mammalian neuron. The data obtained from MALDI and SIMS supported that the signals of small molecules in the low molecular region, such as PC head groups and fatty acids (detected in SIMS) were obtained from the intact lipids (Yang *et al.*, 2010). DESI-IMS has been used for imaging of most commonly encountered brain lipid species such as PE and PI in rat spinal cord cross sections in negative-ion mode. The ion image of PI (38:4) was shown in grey matter regions such as the cortex and hippocampus. The ion image of PE (at m/z 888) showed the white specific region in the brain (Dill *et al.*, 2009).

7.1.2. Sphingolipids

The sphingolipid is a type of lipid obtained from the aliphatic amino alcohol sphingosine. The main functions of sphingolipids are transmission and cell recognition. The investigation of sphingolipids is very important because they are indicative of aging and may function as a disease marker. Sphingolipids contain a sphingoid base backbone and include sphingomyelins (SM), sulfatides (ST), ceramides, cerebrosides, and gangliosides (Merrill *et al.*, 2009) (Figure 13). Changes in the levels of lipids,

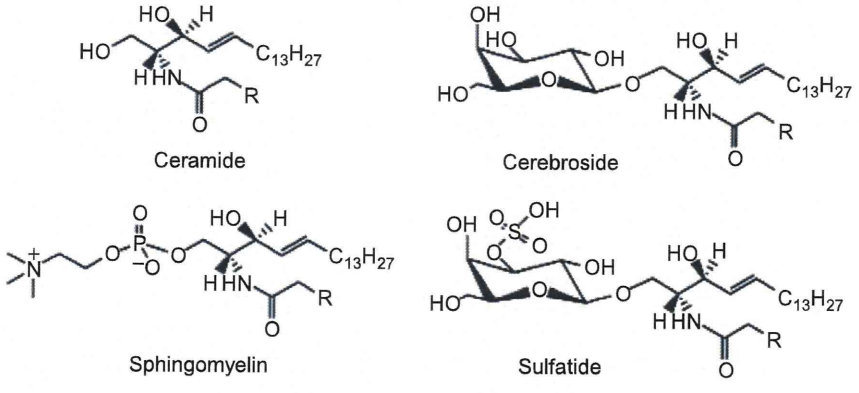

FIGURE 13 Structure of sphingolipids. Reprinted from Jackson and Woods (2009) with permission from Elsevier Science.

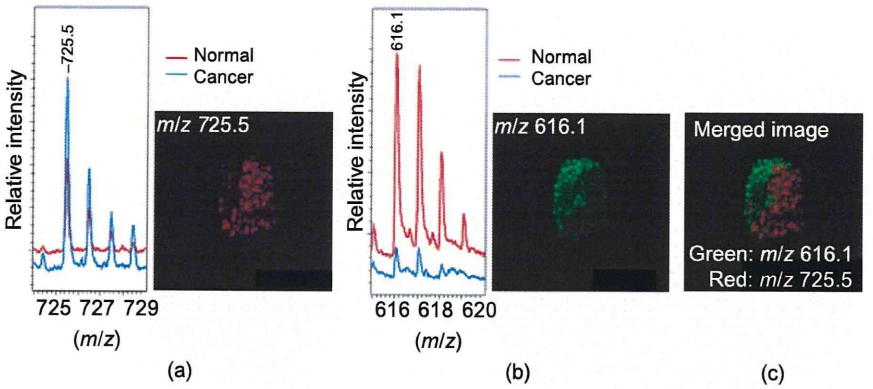

FIGURE 14 Imaging of normal and cancerous cells in human liver sample. (a) The most prominent signal at m/z 725 showed the higher expression for cancerous cells than normal cells. (b) The signal at m/z 616 showed the higher distribution of this molecule in normal cells. (c) Merged images at m/z 725 and 616. Reprinted from Shimma *et al.* (2007) with permission from Elsevier Science.

in particular ceramide, also have been observed in apoptosis or cell death (Fuchs *et al.*, 2007; Thomas *et al.*, 1999). MALDI-MS/MS analyses were used to image liver tissue samples at a thickness 3 μm from a patient with colon cancer. A higher expression of sphingomyelin (SM, 16:0) at m/z 725 was observed in cancerous tissue than in normal tissue by MS/MS analyses (Figure 14). In contrast, a strong distribution of an ion at m/z 616 was observed in the normal but not cancerous tissue sample (Shimma *et al.*, 2007). IMS has also been used to detect seminolipid, a glycolipid synthesized in sperm. Here, seminolipid localization was performed in mice testis during testicular maturation Goto-Inoue *et al.* (2009b). In another study, the distribution pattern of ganglioside molecular species (C-18 and C-20) in mouse hippocampus was demonstrated using MALDI-IMS. The localization of C-18 species was found in the frontal brain and C-20 species contained in the entorhinal-hippocampus projections of the molecular layer (ML) of the dentate gyrus. Figure 15 shows the distribution of C-20-sphingosine–containing gangliosides in the hippocampal formation (Sugiura *et al.*, 2008). In a study using gold NPs in Nano-PALDI-IMS and comparing it with the use of DHB matrix, the PI, ST, and ganglioside species (GM3, GM2, GM1, GD1, and GD3) were all detected with higher sensitivity. This is the first report of the visualization of minor sphingolipids by IMS analyses using gold NPs in tissue sections (Goto-Inoue *et al.*, 2010). Higher expression of sulphatides in ovarian cancer cells was reported compared with a normal sample with MALDI-IMS analysis and similar results were obtained by a transcriptomic approach of lipid analysis (Liu *et al.*, 2010). The high spatial resolution localization of glucosylceramide in spleen of a mouse model of Gaucher disease was

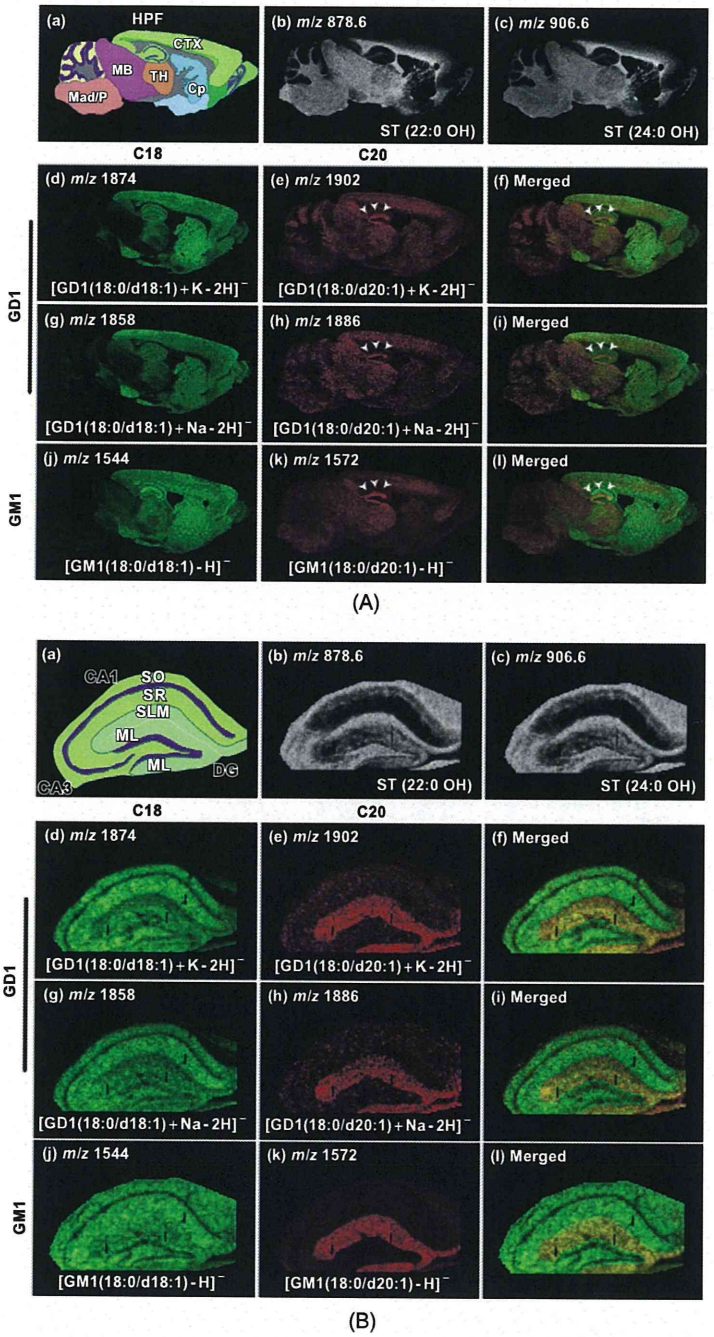

FIGURE 15 (Continued)

FIGURE 15 Localization of C20-sphingosine–containing gangliosides in the hippocampal formation. IMS at 50-mm raster step size was used to gain an overview of ganglioside distribution in different brain regions (A), and IMS at 15-mm raster size was used to study in detail the distribution pattern of gangliosides in the hippocampus (B). In both panels, schematic diagram of the brain section (a) and ion images of STs (b)–(c) are presented. For ions corresponding to the GD1 molecular species, we observed the ion distributions of both sodium and potassium complexes; that is, the ions at m/z 1858 (f) and m/z 1886 (g), which correspond to the $[M+Na-H]^-$ form of C18- and C20-GD1, and those at m/z 1874 (h) and m/z 1902 (i), which correspond to the $[M+K-H]^-$ form of C18- and C20-GD1, respectively. The ion distribution patterns corresponding to the GD1-Na salts and GD1-K salts are fairly uniform for both C18- and C20-species. For GM1, m/z 1544 (d) and m/z 1572 (e), which correspond to C18- and C20-sphingosines–containing GM1, respectively, are shown. HPF, hippocampus formation; MadP, ————————-; CTX, cerebral cortex; MB, ————————-; TH, Thalamus; SO,————————-; SR, stratum radiatum; SLM, stratum lacunosum molecular; ML, molecular layer. Reprinted from Sugiura *et al.* (2008) with permission from Public Library of Science.

also demonstrated using MALDI-IMS (Snel and Fuller, 2010). Ganglioside GM2, asialo-GM2 (GA2), and sulfatides in brain from a mouse model of Tay-Sachs/Sandhoff disease (Chen *et al.*, 2008) and sulfatides in mouse kidney (Marsching *et al.*, 2011) have been reported.

7.1.3. Nonpolar Lipids

Imaging and identification of nonpolar lipid in tissue sections is not easy, perhaps because of the difficulty in the ionization of molecules in MALDI-MS. Thus only a few species of nonpolar lipids have been successfully reported. One example is cholesterol, a highly abundant lipid in many tissues. It is usually detected at m/z 369 after the loss of a water molecule using an organic matrix in MALDI-MS. Cholesterol is a vital constituent of the cell membrane, required for lipid organization and cell signaling. Changes in the quantity of cholesterol in tissue can cause myocardial infarctions and stroke, as well as other disorders (Fernandez *et al.*, 2011). SIMS has been used for imaging of cholesterol with the capability to analyze single cells. In this setup one drawback was that cholesterol was fragmenting (Piehowski *et al.*, 2008). However, the use of NIMS could directly analyze the brain cholesterol metabolites in Smith-Lemli-Opitz syndrome without the fragmentation of molecules in MS (Patti *et al.*, 2010). The distribution of triglycerides (TAG) in mouse embryo was also investigated using MALDI-IMS (Hayasaka *et al.*, 2009). TAG is an ester derived from glycerol and three fatty acids and is the main constituent of vegetable oil and animal fats. Figure 16 is illustrates the distribution of different molecular species of TAG $[(16:0/18:2/18:1)+Na]^+$, $[(16:0/18:1/18:1)+Na]^+$, $[(16:0/20:3/18:1)+K]^+$ in mouse embryo. The ion images of TAG were concentrated mainly around the brown adipose and liver tissue (Hayasaka *et al.*, 2009).

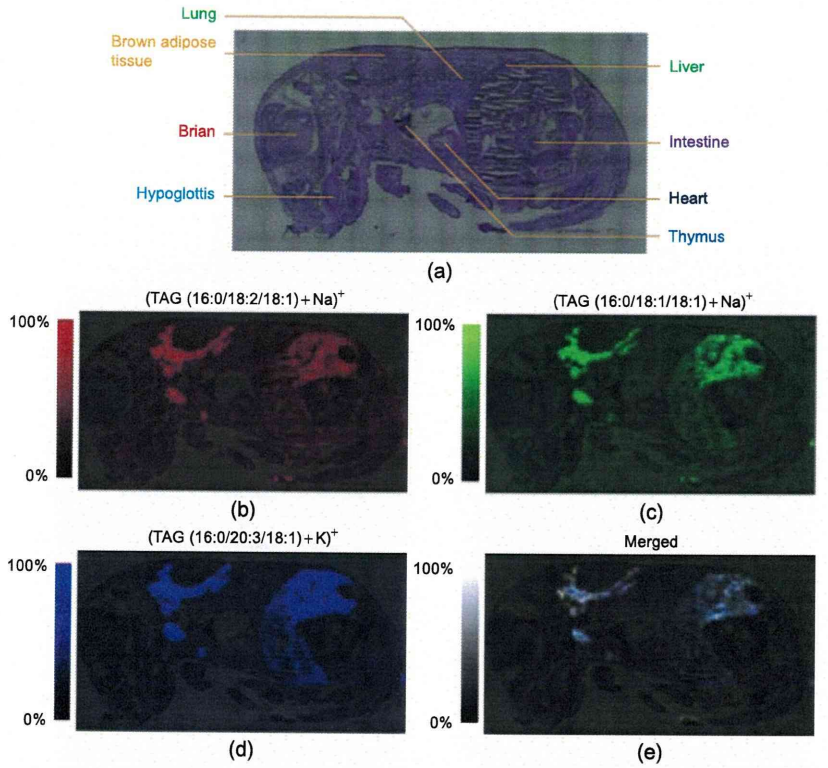

FIGURE 16 MALDI-IMS of neutral lipids. Distribution of triglycerides (TAG) in mouse embryo. (a) H&E staining, (b) ion images of [TAG (16:0/18:2/18:1)+Na]$^+$, [TAG 16:0/18:1/18:1)+Na]$^+$, and [TAG (16:0/20:3/18:1)+K]$^+$ are shown. (b)–(d) The ion images were merged with the optical image of an H&E-stained section. (e) Three merged TAG images demonstrate the same distribution. Reprinted from Hayasaka *et al.* (2009) with permission from Springer.

7.2. IMS for Proteomics

The study of proteomics is useful for biomarker discovery of a large number of diseases, using tissue samples such as vascular tissue, heart, brain, lung or bone, with a current major focus on cancer and malignant tissues (MacAleese *et al.*, 2009). Today MALDI-IMS is increasingly being used for direct analysis of peptides and proteins from tissue sections; the main advantage is that it requires no labeling reagents (McDonnell and Heeren, 2007; Stoeckli *et al.*, 2001). Immunohistochemistry (IHC) has long been the standard technology for imaging of peptide and protein distribution in tissue. The sensitivity of IHC is usually excellent. However, this method requires a specific binder, usually an antibody, to detect a previously defined protein from the sample. Only a very small number of molecules may be detected in parallel, and these all need to be known beforehand.